Cone-beam local reconstruction based on a Radon inversion transformation*

Wang Xian-Chao(汪先超), Yan Bin(闫 镔)†, Li Lei(李 磊), and Hu Guo-En(胡国恩)

National Digital Switching System Engineering and Technological Research Center, Zhengzhou 450002, *China*

(Received 28 April 2012; revised manuscript received 24 May 2012)

The local reconstruction from truncated projection data is one area of interest in image reconstruction for computed tomography (CT), which creates the possibility for dose reduction. In this paper, a filtered-backprojection (FBP) algorithm based on the Radon inversion transform is presented to deal with the three-dimensional (3D) local reconstruction in the circular geometry. The algorithm achieves the data filtering in two steps. The first step is the derivative of projections, which acts locally on the data and can thus be carried out accurately even in the presence of data truncation. The second step is the nonlocal Hilbert filtering. The numerical simulations and the real data reconstructions have been conducted to validate the new reconstruction algorithm. Compared with the approximate truncation resistant algorithm for computed tomography (ATRACT), not only it has a comparable ability to restrain truncation artifacts, but also its reconstruction efficiency is improved. It is about twice as fast as that of the ATRACT. Therefore, this work provides a simple and efficient approach for the approximate reconstruction from truncated projections in the circular cone-beam CT.

Keywords: computed tomography, image reconstruction, truncated data, Radon inversion transform

PACS: 87.59.–e, 07.85.–m **DOI:** 10.1088/1674-1056/21/11/118702

1. Introduction

Cone-beam X-ray computed tomography (CT) has been widely applied to many fields, especially in nondestructive testing and medical applications.[1,2] Practically-available flat-panel volumetric CT scanners can provide 3D images from projections obtained during a single rotation of the system around the stationary object.[3,4] In most such scanners, the 3D image reconstruction is carried out using analytical filtered-backprojection (FBP) algorithms,[5,6] among which the Feldkamp–Davis–Kress (FDK) algorithm is the most popular one and gives reasonably good results in case of small cone angle and no truncation in the transverse direction.[7]

When the projections are truncated, particularly when only a portion of the entire width of the object is captured during acquisition, achieving high image quality becomes more difficult. The truncated projections can be caused by limitations of the detector size, but also by a narrow collimation of the X-ray beam just to the local region. The local reconstruction has many practical applications, such as dose reduction. However, the straightforward application of the conventional FBP algorithm on the truncated data typically causes significant image artifacts in the reconstruction results close to the boundary of the scanning field of view (SFOV).

While some specific scenarios of truncation still allow accurate reconstructions using dedicated analytical reconstruction methods,[8−12] the other truncation cases can only be solved in practice using approximate methods. The most common approach is to extrapolate in each projection image the measured values explicitly beyond the image boundaries in case of truncation and to perform the conventional reconstruction from the extrapolated projections.[13,14] In 2011, Dennerlein did interesting research and developed an approximate truncation resistant algorithm for computed tomography (ATRACT) using the Laplace operator, which achieved similar results to that of the extrapolation methods in case of data truncation.[15] Although the ATRACT does not require an explicit extrapolation of the projection data, its data filtering comprises the complex implementation of Radon transform and backprojection, and its calculation cost is approximately twice as large as that of the FDK algorithm.

In this paper, we propose an FBP algorithm based

*Project supported by the National High Technology Research and Development Program of China (Grant No. 2012AA011603).
†Corresponding author. E-mail: ybspace@yahoo.com.cn
© 2012 Chinese Physical Society and IOP Publishing Ltd

on the Radon inversion transform (RIT) that does not require an explicit extrapolation of the projection data, but nevertheless achieves similar results as those of the extrapolation methods and the ATRACT in case of data truncation. Its reconstruction efficiency has an improvement over the ATRACT and is equivalent to the FDK algorithm.

This paper is organized as follows. In Section 2, the FBP algorithm based on the RIT is introduced in detail. In Section 3, the advantages of the proposed algorithm are demonstrated by the results of numerical simulation and real data reconstruction compared with the FDK algorithm and the ATRACT. Finally, Section 4 contains the conclusion.

2. Reconstruction theory

2.1. Geometry and notation

As shown in Fig. 1, the presentation in this paper is based on the planar, circular acquisition geometry with a flat detector. We denote the density function by $f(\boldsymbol{r})$, $\boldsymbol{r} = (x, y, z)$ and assume that the X-ray source moves along the trajectory $\boldsymbol{a}(\lambda) = (R\cos\lambda, R\sin\lambda, 0)$, where S, R, and λ denote the distance between the source and the detector, the scanning radius, and the scanning angle, respectively. Projection data are acquired with a planar 2D detector, which is parallel to vectors $\hat{\boldsymbol{e}}_u(\lambda) = (-\sin\lambda, \cos\lambda, 0)$, $\hat{\boldsymbol{e}}_v(\lambda) = (0, 0, 1)$ and orthogonal to $\hat{\boldsymbol{e}}_w(\lambda) = (\cos\lambda, \sin\lambda, 0)$. Points on the detector are specified using (u, v), where u and v are the coordinates measured along axes $\hat{\boldsymbol{e}}_u(\lambda)$ and $\hat{\boldsymbol{e}}_v(\lambda)$, respectively.

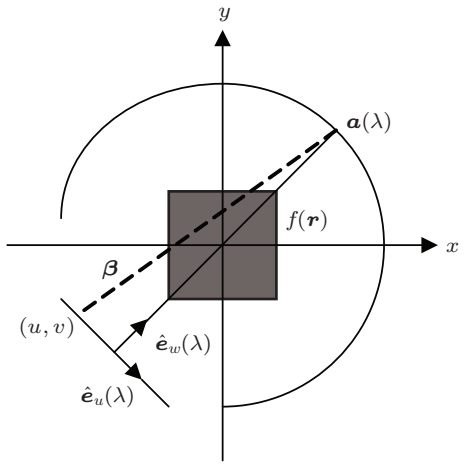


Fig. 1. The 3D circular cone-beam acquisition geometry with a flat detector.

The projection data $g(\lambda, u, v)$ can be written as

$$g(\lambda, u, v) = \int_0^\infty f(\boldsymbol{a}(\lambda) + t\boldsymbol{\beta}(\lambda, u, v))\mathrm{d}t, \quad (1)$$

where $\boldsymbol{\beta}(\lambda, u, v)$ is the unit direction vector of the ray connecting $\boldsymbol{a}(\lambda)$ with the point (u, v) on the detector plane.

2.2. FDK algorithm

The FDK algorithm is a popular approximate FBP-type algorithm for tomographic image reconstruction in the circular cone-beam geometry described above. The FDK algorithm computes an estimate $f^{(\mathrm{FDK})}(\boldsymbol{r})$ of the object function $f(\boldsymbol{r})$ by back-projecting filtered projection data g_F according to

$$f^{(\mathrm{FDK})}(\boldsymbol{r}) = \int_0^{2\pi} \frac{RS}{[R - \boldsymbol{r}\cdot\hat{\boldsymbol{e}}_w(\lambda)]^2} g_\mathrm{F}(\lambda, u^*, v^*)\mathrm{d}\lambda, \quad (2)$$

where u^* and v^* denote the coordinates of the projection of $\boldsymbol{r}$ onto the detector and can be written as

$$u^* = \frac{S\boldsymbol{r}\cdot\hat{\boldsymbol{e}}_u}{R - \boldsymbol{r}\cdot\hat{\boldsymbol{e}}_w}, \quad v^* = \frac{Sz}{R - \boldsymbol{r}\cdot\hat{\boldsymbol{e}}_w}. \quad (3)$$

The g_F is defined for the transaxially non-truncated data as

$$g_\mathrm{F}(\lambda, u, v) = \int_{-\infty}^{\infty} h_\mathrm{R}(u - u')g_1(\lambda, u', v)\mathrm{d}u', \quad (4)$$

where h_R denotes the ramp filter kernel.[16] The function g_1 corresponds to the weighted projection data

$$g_1(\lambda, u, v) = \frac{S}{\sqrt{S^2 + u^2 + v^2}} g(\lambda, u, v). \quad (5)$$

From the course of the FDK algorithm, we can see that the error only emerges in the filtering processing when the projection data are transaxially truncated. The error will be bigger when the position of the filtered value is nearer the boundary of the truncated projection data. So the truncation artifacts appear as bright bands and streaks at the edges of SFOV in z-axial reconstruction slices.

2.3. FBP algorithm based on RIT

According to Ref. [17], the ramp and the Hilbert filterings have the following relationship:

$$g_\mathrm{F}(\lambda, u, v) = \frac{1}{2\pi}\frac{\partial}{\partial u} g_\mathrm{H}(\lambda, u, v), \quad (6)$$

where g_H denotes the 1D convolutions of the weighted projection data with the Hilbert kernel h_H and can be written as

$$g_\mathrm{H}(\lambda, u, v) = \int_{-\infty}^{\infty} h_\mathrm{H}(u - u')g_1(\lambda, u', v)\mathrm{d}u'. \quad (7)$$

So

$$g_{\mathrm{F}}(\lambda,u,v) = \frac{1}{2\pi}\frac{\partial}{\partial u}\int_{-\infty}^{\infty} h_{\mathrm{H}}(u-u')g_1(\lambda,u',v)\mathrm{d}u' = \frac{1}{2\pi}\int_{-\infty}^{\infty} h_{\mathrm{H}}(u')\frac{\partial}{\partial u}g_1(\lambda,u-u',v)\mathrm{d}u'. \quad (8)$$

In the case of 2D reconstruction, the application of the filter operation (8) together with Eqs. (2) and (5) is the 2D Radon inversion transform. In the following, we extend the 2D Radon inversion transform to reconstruct 3D images, and then obtain the FBP algorithm based on the Radon inversion transform, which can be written as follows.

Step 1 Weighting the projection data as in Eq. (5)

$$g_1(\lambda,u,v) = \frac{S}{\sqrt{S^2+u^2+v^2}}g(\lambda,u,v). \quad (9)$$

Step 2 Differentiation of g_1 with respect to u (local operation)

$$g_2(\lambda,u,v) = \frac{\partial}{\partial u}g_1(\lambda,u,v). \quad (10)$$

Step 3 The Hilbert filtering of g_2 (global operation)

$$g_3(\lambda,u,v) = \frac{1}{2\pi}g_2(\lambda,u,v)h_{\mathrm{H}}(u). \quad (11)$$

Step 4 Backprojecting the filtered cone-beam projections onto the 3D image

$$f^{(\mathrm{RIT})}(\boldsymbol{r}) = \int_0^{2\pi}\frac{RS}{\left[R-\boldsymbol{r}\cdot\hat{\boldsymbol{e}}_w(\lambda)\right]^2}g_3(\lambda,u^*,v^*)\mathrm{d}\lambda, \quad (12)$$

where u^* and v^* have been described in Eq. (3).

Note that $f^{(\mathrm{FDK})}$ and $f^{(\mathrm{RIT})}$ are mathematically identical for non-truncated cone-beam data, but the FBP algorithm based on the RIT and the FDK algorithm perform differently for image reconstructions from the truncated data. An intuitive reason for that is that the filtering operation in the new FBP formula consists of a purely local component and a subsequent global component. The local component in Eq. (10) produces the intermediate function g_2 that can be obtained accurately for all points in the detector, even in the presence of data truncation. The data truncation thus only affects the integration in Eq. (11) and yields an approximate filtered projection g_3. Note, furthermore, that the values of g_2 are much more closely distributed around 0 in most regions than those of g_1. Therefore, the restriction of the integration domain in Eq. (11) does not significantly change the outcome of the total filter operation. From the above analysis to the FBP algorithm based on the RIT, it is found that the proposed algorithm has the ability to restrain truncation artifacts in case of data truncation. At the same time, the data filtering of the proposed algorithm is simple like that in the FDK algorithm, and thus its reconstruction efficiency is improved over the ATRACT.

3. Implementation and experimental results

To show the advantages of the presented FBP algorithm based on the RIT, we implemented it in C language, and evaluated it with both numerical simulation data and real CT data. The CPU used to implement the experiments is Intel Xeon(R) X5450 @ 3.00 GHz.

3.1. Simulation studies

To compare the proposed algorithm with the FDK algorithm and the ATRACT, we performed them and evaluated the results with 256×256×256 standard 3D Shepp–Logan head phantom.[18,19] In the circular cone-beam configuration, the trajectory had a radius of 477 mm and a source–detector distance of 1265 mm. The cone-beam projection data was generated with 360 projection views uniformly distributed over the 2π circular trajectory, and its size was 256×256. Firstly, we used the FDK, the ATRACT, and the proposed algorithm to reconstruct the model with non-truncated data. Secondly, we reconstructed the center inner region (160×160×160) with truncated data (160×160).

To evaluate the reconstruction results, the root of the mean square errors (RMSE) is introduced and can be written as[20]

$$\mathrm{RMSE} = \sqrt{\frac{1}{N}\sum_{i=1}^{N}[f_{\mathrm{t}}(i)-f_0(i)]^2}, \quad (13)$$

where f_{t} and f_0 denote the reconstructed and the reference images of N voxels, respectively.

In Fig. 2, we display 2D z-axial slices in 3D images reconstructed using the FDK algorithm, the ATRACT, and the the proposed algorithm with non-truncated data. From Fig. 2 and the RMSE shown in Table 1, we can see that the FDK algorithm, the ATRACT, and the proposed algorithm reconstruct

images with little difference in the case of the non-truncated data. According to the cost shown in Table 1, the reconstruction efficiencies of the FDK and the proposed algorithms are fast, while that of the ATRACT is slow. The reason is that the filtering processing of the ATRACT is composed of the Radon transform and backprojection calculation, and its implementation is heavy. The calculation cost of the ATRACT is nearly twice as large as that of the proposed algorithm.

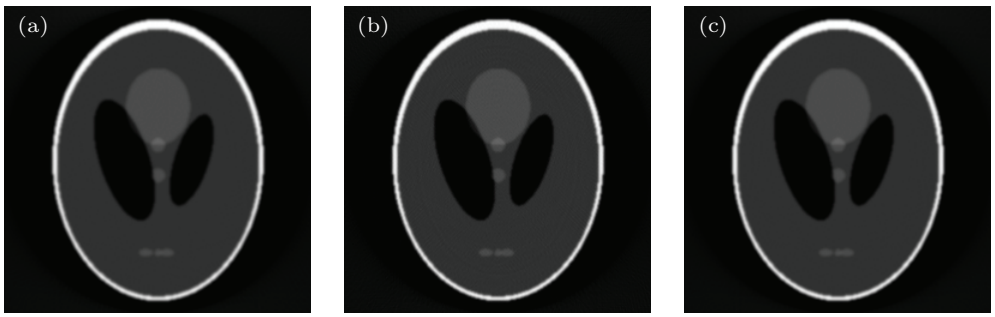


Fig. 2. The 2D z-axial slices in 3D images reconstructed using (a) the FDK algorithm, (b)the ATRACT, and (c) the proposed algorithm with non-truncated data.

Table 1. The cost and RMSE for the reconstructions in Fig. 2.

Algorithm	Reconstruction size/pixel	Reconstruction cost/min	RMSE
FDK algorithm	256×256×256	24.62	0.0066
ATRACT	256×256×256	42.92	0.0076
The proposed algorithm	256×256×256	24.59	0.0068

In Fig. 3, we display 2D z-axial slices in 3D images reconstructed using the FDK algorithm, the ATRACT, and the proposed algorithm with truncated data. From Fig. 3 and the RMSE shown in Table 2, we find that the truncation artifacts are severe in the images reconstructed by the FDK algorithm, but the ATRACT and the proposed algorithm can restrain the truncation artifacts efficiently. From the cost shown in Table 2, the proposed algorithm is fast like the FDK algorithm, but the reconstruction efficiency of the ATRACT is slow. The calculation cost of the ATRACT is about twice as large as that of the proposed algorithm.

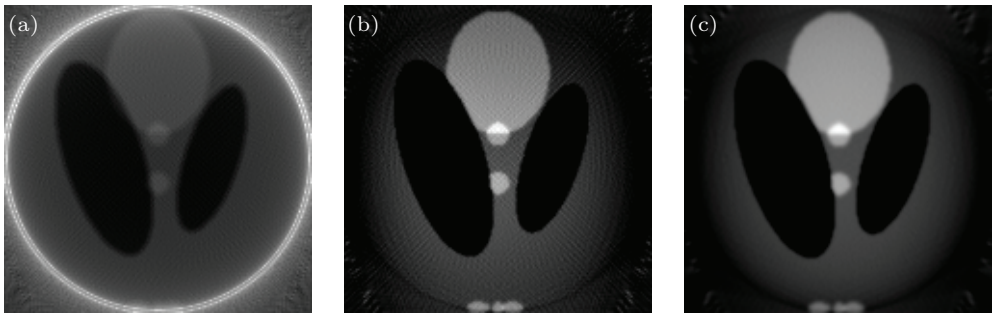


Fig. 3. The 2D z-axial slices in 3D images reconstructed using (a) the FDK algorithm, (b) the ATRACT and (c) the proposed algorithm with truncated data.

Table 2. The cost and RMSE for the reconstructions in Fig. 3.

Algorithm	Reconstruction size/pixel	Reconstruction cost/min	RMSE
FDK algorithm	160×160×160	6.15	0.18
ATRACT	160×160×160	12.83	0.016
The proposed algorithm	160×160×160	6.13	0.015

3.2. Reconstruction using real data

To further check the capability of the proposed algorithm, we carried out experiments to reconstruct a local region of human head phantom from the truncated real data. The real data was acquired with a cone-beam CT system, which was mainly constitutive of an X-ray source (Hawkeye 130, Thales, France), an orthogonally rotary stage with an object holder, and a flat-panel detector (Varian 4030E, USA) with a pixel size of 0.127 mm. In the circular cone-beam configuration, the trajectory had a radius of 678 mm and a source–detector distance of 1610 mm. The size of the reconstructed region was 600×600×600 with a pixel size 0.107 mm. The cone-beam data was generated with 360 projection views uniformly distributed over the 2π circular trajectory.

As shown in Fig. 4, we use the FDK algorithm to reconstruct the local region from non-truncated and truncated data respectively. Figure 4(a) shows the 376th z-axial reconstructed slice with non-truncated data. Figure 4(b) shows the 376th z-axial reconstructed slice with truncated data visualized in the window [0,1]. Because of the severe truncation artifacts, the reconstructed image is very obscure and cannot be identified. We modify the display window to [0, 0.3] in Fig. 4(c). The quality of the reconstructed image is improved in the center region, but the truncation artifacts still exist at the boundary of the local region and cause the boundary obscure.

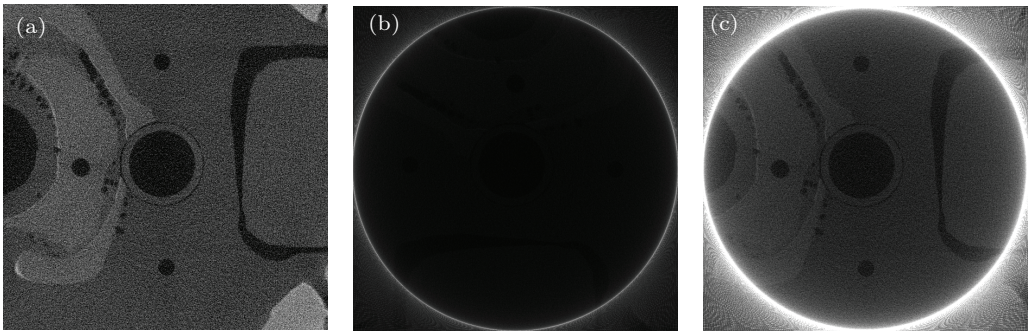


Fig. 4. The 376th z-axial slices in 3D images reconstructed by the use of the FDK algorithm: (a) the 376th slice from non-truncated data visualized in the window [0,1]; (b) the 376th slice from truncated data visualized in the window [0,1]; (c) the 376th slice from truncated data visualized in the window [0, 0.3].

From the reconstruction results using real data shown in Fig. 5, we find that the proposed algorithm can effectively restrain the truncation artifacts like the ATRACT with the truncated data, so its resistant ability to truncation artifacts is also demonstrated by the real data reconstruction. Furthermore, the ATRACT and the proposed algorithm react to the truncation with a globally almost constant offset on the reconstructed densities, and this offset can be nicely compensated by adapting the grayscale window during visualization. From the reconstruction cost shown in Table 3, the proposed algorithm is improved over the ATRACT, and is more than two times faster than it. We can see that the reconstruction efficiency advantage of the proposed algorithm will be more obvious when the reconstruction size is larger.

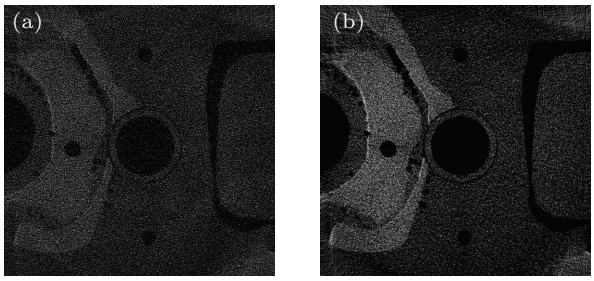


Fig. 5. The 376th z-axial slices in 3D images reconstructed by using the ATRACT and the proposed algorithm with truncated data: (a) the reconstruction result of ATRACT visualized in the window [0,1]; (b) the reconstruction result of the proposed algorithm visualized in the window [0,1].

Table 3. The cost for the reconstructions in Fig. 5.

Algorithm	Reconstruction size/pixel	Reconstruction cost/min
ATRACT	600×600×600	454.35
The proposed algorithm	600×600×600	182.65

4. Conclusion

In the various applications of CT, it is common that the size of the detector is limited and that of the reconstructed object is relatively large, thereby causing the projection data to be truncated at all directions. In this paper, we have presented an approximate truncation resistant algorithm for the image reconstruction from the truncated projection data in the circular cone-beam CT. The algorithm is an FBP algorithm based on the Radon inversion transform. Its data filtering contains the derivative of projections (local operation) and the subsequent Hilbert filtering (global operation). Its local operation of the differentiation of projections shows a resemblance to the ATRACT, which is the reason that the proposed algorithm can restrain the truncation artifacts. From the experimental results, we find that the proposed algorithm has the same ability to restrain the truncation artifacts as the ATRACT in the local reconstruction; Furthermore, it is fast like the FDK algorithm, and about two times faster than the ATRACT. In conclusion, the proposed algorithm provides a simple and efficient approach to solve approximate local reconstruction problems with truncated projection data in the circular cone-beam CT.

References

[1] Luo Z Y, Yang X Q, Meng Y Z and Deng Y 2010 *Acta Phys. Sin.* **59** 8237 (in Chinese)

[2] Zhou G Z, Tong Y J, Chen C, Ren Y Q, Wang Y D and Xiao T Q 2011 *Acta Phys. Sin.* **60** 028071 (in Chinese)

[3] Zhu S P, Tian J, Yan G R, Qin C H and Feng J C 2009 *International Journal of Biomedical Imaging* 960573

[4] Jia P X, Zhang F, Yan B and Bao S L 2010 *Chin. Phys.* B **19** 087802

[5] Kak A C and Slaney M 1987 *Principles of Computerized Tomographic Imaging* (New York: IEEE Press)

[6] Wang X C, Li L, Yu C Q, Yan B and Bao S L 2012 *J. X-ray Sci. Tech.* **20** 69

[7] Feldkamp L A, Davis L C and Kress J W 1984 *J. Opt. Soc. Am.* A **1** 612

[8] Clackdoyle R, Noo F, Guo J Y and Roberts J A 2004 *IEEE Trans. Nucl. Sci.* **51** 2570

[9] Zhuang T L, Leng S, Nett B E and Chen G H 2004 *Phys. Med. Biol.* **49** 5489

[10] Yu L F, Zou Y, Sidky E Y, Pelizzari C A, Munro P and Pan X C 2006 *IEEE Trans. Med. Imag.* **25** 869

[11] Dennerlein F, Noo F, Schoendube H, Hornegger J and Lauritsch G 2008 *IEEE Trans. Med. Imag.* **27** 887

[12] Xia D, Cho S and Pan X C 2009 *J. X-ray Sci. Tech.* **17** 189

[13] Hsieh J, Chao E, Thibault J, Grekowicz B, Horst A, McOlash S and Myers T J 2004 *Med. Phys.* **31** 2385

[14] Ohnesorge B, Flohr T, Schwarz K, Heiken J P and Bae K T 2000 *Med. Phys.* **27** 39

[15] Dennerlein F 2011 *11th International Meeting on Fully Three-Dimensional Image Reconstruction in Radiology and Nuclear Medicine* July 11–15, 2011 Potsdam, Germany, p. 80

[16] Wei Y C and Wang G 2005 *Computers and Mathematics with Applications* **49** 731

[17] Noo F, Defrise M, Clackdoyle R and Kudo H 2002 *Phys. Med. Biol.* **47** 2525

[18] Shepp L A and Logan B F 1974 *IEEE Trans. Nucl. Sci.* **21** 21

[19] Wang L Y, Li L, Yan B, Jiang C S, Wang H Y and Bao S L 2010 *Chin. Phys.* B **19** 088106

[20] Han X, Bian J G, Eaker D R, Kline T L, Sidky E Y, Ritman E L and Pan X C 2011 *IEEE Trans. Med. Imag.* **30** 606